General Disclaimer

One or more of the Following Statements may affect this Document

- This document has been reproduced from the best copy furnished by the organizational source. It is being released in the interest of making available as much information as possible.

- This document may contain data, which exceeds the sheet parameters. It was furnished in this condition by the organizational source and is the best copy available.

- This document may contain tone-on-tone or color graphs, charts and/or pictures, which have been reproduced in black and white.

- This document is paginated as submitted by the original source.

- Portions of this document are not fully legible due to the historical nature of some of the material. However, it is the best reproduction available from the original submission.

Produced by the NASA Center for Aerospace Information (CASI)

NASA Technical Memorandum 74080

A FINITE ELEMENT SIMULATION OF SOUND ATTENUATION IN A FINITE DUCT WITH A PERIPHERALLY VARIABLE LINER

(NASA-TM-74080) A FINITE ELEMENT SIMULATION OF SOUND ATTENUATION IN A FINITE DUCT WITH A PERIPHALLY VARIABLE LINER (NASA) 41 p HC A03/MF A01 CSCL 20A
N78-11798
Unclas
G3/71 52813

WILLIE R. WATSON

October 1977

National Aeronautics and Space Administration
Langley Research Center
Hampton, Virginia 23665

DEC 1977
RECEIVED
NASA STI FACILITY

A FINITE ELEMENT SIMULATION OF SOUND ATTENUATION IN A FINITE DUCT WITH A PERIPHERALLY VARIABLE LINER

by

Willie R. Watson
NASA-Langley Research Center
Hampton, VA

Using multimodal analysis, a variational finite element method is presented for analyzing sound attenuation in a three-dimensional finite duct with a peripherally variable liner in the absence of flow. A rectangular element, with cubic shape functions, is employed. Excellent comparison between exact results and the finite element method is obtained in cases where an analytical solution exists. This study indicates that, once a small portion of a peripheral liner is removed, the attenuation rate near the frequency where maximum attenuation occurs drops significantly. Also, it was observed that the positioning of the liner segments affects the attenuation characteristics of the liner and that effects of the duct termination are important in the low frequency ranges. In general, the results indicate that the main effect of peripheral variation of the liner is a broadening of the attenuation characteristics in the mid-frequency range. Finally, it is concluded that, due to matrix size limitations of the presently available computer program, the eigenvalue equations should be solved out of core in order to handle realistic sources.

A FINITE ELEMENT SIMULATION OF SOUND ATTENUATION IN A FINITE DUCT WITH A PERIPHERALLY VARIABLE LINER

by

Willie R. Watson
NASA-Langley Research Center
Hampton, VA

Using multimodal analysis, a variational finite element method is presented for analyzing sound attenuation in a three-dimensional finite duct with a peripherally variable liner in the absence of flow. A rectangular element, with cubic shape functions, is employed. Excellent comparison between exact results and the finite element method is obtained in cases where an analytical solution exists. This study indicates that, once a small portion of a peripheral liner is removed, the attenuation rate near the frequency where maximum attenuation occurs drops significantly. Also, it was observed that the positioning of the liner segments affects the attenuation characteristics of the liner and that effects of the duct termination are important in the low frequency ranges. In general, the results indicate that the main effect of peripheral variation of the liner is a broadening of the attenuation characteristics in the mid-frequency range. Finally, it is concluded that, due to matrix size limitations of the presently available computer program, the eigenvalue equations should be solved out of core in order to handle realistic sources.

SYMBOLS

$\bar{A}_o, \bar{A}_1, \bar{A}_2, \bar{A}_3$	coefficients in polynomial representation to β (eqns. 21 and 22)
A_n, B_n	modal amplitudes (see eq. 3)
$\tilde{A}_{mn}(z)$	$= K_m(A_m e^{iK_m z} - B_m e^{-iK_m z})(A_n^* e^{-iK_n^* z} + B_n^* e^{iK_n^* z})$
c	ambient speed of sound
c_n	$= [(K_n/K\beta_e^{-1})/(K_n/K\beta_e^{+1})]e^{2iK_n d}$
d, ℓ, h	length, width and height of the duct of figure 1, respectively
D_n	$= \int_0^{\ell}\int_0^{h} GF_n dxdy$
[D], [S], [M]	square matrices (equation (13))
E_z	$= \int_0^{h}\int_0^{\ell} I_z dydx$
$f_1(\xi)$, $f_2(\xi)$	cubic shape functions (equation 10)
$F_n(x,y)$	acoustic mode in duct cross section (eq. 4)
$F_{mn}(x,y)$	$= [\cos \gamma_n x - \frac{ik\beta_3}{\gamma_n} \sin \gamma_n x][\cos \alpha_m y - \frac{ik\beta_1}{\alpha_m} \sin \alpha_m y]$
G(x,y)	acoustic pressure distribution at entrance plane (equation 2c)
G_{IJ}^{PQ}	nodal values of G(x,y) and its first and mixed partial derivatives

ORIGINAL PAGE IS
OF POOR QUALITY

SYMBOLS

$\bar{A}_o, \bar{A}_1, \bar{A}_2, \bar{A}_3$	coefficients in polynomial representation to β (eqns. 21 and 22)
A_n, B_n	modal amplitudes (see eq. 3)
$\tilde{A}_{mn}(z)$	$= K_m(A_m e^{iK_m z} - B_m e^{-iK_m z})(A_n^* e^{-iK_n^* z} + B_n^* e^{iK_n^* z})$
c	ambient speed of sound
c_n	$= [(K_n/K\beta_e - 1)/(K_n/K\beta_e + 1)]e^{2iK_n d}$
d, ℓ, h	length, width and height of the duct of figure 1, respectively
D_n	$= \int_0^{\ell}\int_0^{h} GF_n dxdy$
[D], [S], [M]	square matrices (equation (13))
E_z	$= \int_0^{h}\int_0^{\ell} I_z dydx$
$f_1(\xi)$, $f_2(\xi)$	cubic shape functions (equation 10)
$F_n(x,y)$	acoustic mode in duct cross section (eq. 4)
$F_{mn}(x,y)$	$= [\cos \gamma_n x - \frac{ik\beta_3}{\gamma_n} \sin \gamma_n x][\cos \alpha_m y - \frac{ik\beta_1}{\alpha_m} \sin \alpha_m y]$
G(x,y)	acoustic pressure distribution at entrance plane (equation 2c)
G_{IJ}^{PQ}	nodal values of G(x,y) and its first and mixed partial derivatives

ORIGINAL PAGE IS
OF POOR QUALITY

I, J, M, N, m P, Q	integers
II	$= \iint_A [\vec{\nabla}F \cdot \vec{\nabla}F - \lambda^2 F^2]\, dA - iK \int_c \beta F^2 dc$
$\overline{II}$	finite element approximation to II
I_z	Axial acoustic intensity (eqn. 5)
i	$= \sqrt{-1}$
k	$= \omega/c$
k_o	k value at which a Cremer liner is tuned
K_n	axial propagation constant
x, y, z	distances along the X, Y, and Z axes respectively
x_I, y_J	respective values of x and y at node (I, J)
t	time
α_m, γ_n	characteristic numbers (eqn. 18(b))
δ	first variation
ζ_I	$= (x - x_I)/\Delta x$
η_J	$=(y - y_J)/\Delta y$
ρ_o	ambient density of air

F_{ij}^{PQ}	unknown nodal values of F and its higher derivatives
β, β_n, β_e	specific admittances
β_{IJ}^{PQ}	nodal values of β and its higher derivatives along the periphery of the duct
Δx, Δy	respective height and length of a finite element (see Figure 2)
ω	angular frequency
λ_n	$= \sqrt{k^2 - k_n^2}$
λ_{mn}	$= \sqrt{\gamma_n^2 + \alpha_m^2}$
ψ_{mn}	$= \int_0^\ell \int_0^h F_m F_n \, dxdy$
$\tilde{\psi}_{mn}$	$= \int_0^\ell \int_0^h F_m F^*_n \, dxdy$
Ω_n	$= \frac{D_n}{\psi_{nn}}$
ΔdB	attenuation rate in decibels
$\{F\}$	vector containing the unknown nodal values of F(x,y) and its higher derivatives
$\{G\}$	vector containing the known values of G(x,y) at the nodes of the entrance plane

ORIGINAL PAGE IS
OF POOR QUALITY

$\vec{\nabla}$	differential vector operator in two dimensions
∇^2	$= \vec{\nabla} \cdot \vec{\nabla}$
$\frac{\partial}{\partial \bar{n}}$	first derivative in normal direction

INTRODUCTION

Lining the interior surfaces of aircraft engine ducts with acoustic treatment is a well established method for reducing internally generated aircraft engine noise. Large commerical aircraft such as the L-1011, DC-10 and Boeing 747 have successfully passed FAA certifications due, in part, to this concept and are positive evidence that acoustic liners can reduce aircraft noise effectively. However, increasingly stringent noise reduction goals require that these acoustic suppression techniques be continually refined and updated. Aircraft companies are now more than ever before in need of new ideas and methods to enhance the present state of liner technology.

Initially, liner research was centered around uniform liners (ref. 1). Later, Zorumski and Lansing (ref. 2) realized that liners could be made more effective by taking advantage of impedance changes in axial segments. In light of this development, Zorumski (ref. 3) developed a theory to compute the attenuation in axially segmented circular and annular ducts. Several other investigators (ref. 4, 5, 6, 7 and 8) have since investigated axially segmented duct liners and their practical application.

The present analysis was motivated, primarily, by the success of axially segmented liners and the desire for further effective methods for minimizing internally generated aircraft noise. In this work, a new type of liner variation, the peripherally variable liner, is investigated. In this type of liner, the impedance of the liner is allowed to vary around the duct perimeter, but remains constant in the axial direction. The impedance boundary conditions for a peripherally variable liner become boundary

ORIGINAL PAGE IS
OF POOR QUALITY

conditions with variable coefficients and an exact analytical solution for the acoustic field cannot be determined.

In this work, a finite element method is employed to extract the acoustic field and calculate sound attenuation in a three-dimensional rectangular duct with a peripherally variable liner. First, the governing Helmholtz equation and impedance boundary condition for zero mean flow are transformed into a single function, Π, which has the governing Helmholtz equation and impedance boundary conditions as its stationary conditions. Next, the finite element method is applied to approximate the functional Π. Cubic functions which insure continuity of acoustic pressure and particle velocity throughout the duct are employed as shape functions. The requirement that the functional Π be stationary results in a set of matrix equations which are solved to obtain the acoustic modes. Source and termination effects due to finite duct length are also included.

ANALYSIS

In this section, the mathematical expressions necessary for evaluation of the attenuation of peripherally variable liners will be developed.

Statement of the Problem

The duct to be analyzed and the Cartesian coordinate system to be used are shown in figure 1. The length, height, and width of the duct are d, h, and ℓ respectively. The duct walls are acoustically lined with a specific acoustic admittance, $\beta(x,y)$, which is independent of the axial coordinate z, but is a function of position along the duct perimeter so that:

$$\begin{bmatrix} \beta(x,0) \\ \beta(x,\ell) \\ \beta(0,y) \\ \beta(h,y) \end{bmatrix} = \begin{bmatrix} \beta_1(x) \\ \beta_2(x) \\ \beta_3(y) \\ \beta_4(y) \end{bmatrix} \tag{1}$$

A constant exit admittance, β_e, is specified at the exit plane ($z = d$), and an acoustic pressure distribution, $G(x,y)$, is input at the entrance plane, ($z = 0$).

In separable geometries with constant values of β on the duct perimeter the solution to the acoustic field is given in terms of known trigometric functions. However, when β is a function of position along the duct perimeter, the solution for the acoustic field must be determined numerically. This paper is primarily concerned with analyzing the variable case. Since existing mathematical models cannot handle this situation, this represents a major contribution of this paper.

Acoustic Equations and Boundary Conditions

Steady state acoustic waves propagating in finite ducts, such as shown in figure 1, are governed by the three-dimensional Helmholtz equation

$$\nabla^2 p + k^2 p = 0 \tag{2a}$$

where $k = \omega/c$ is the wave number, p is the acoustic pressure, ω is the angular frequency and c is the speed of sound. The acoustic boundary condition along the duct perimeter is given in the form

$$\frac{\partial p}{\partial \bar{n}} - ik\beta p = 0 \tag{2b}$$

ORIGINAL PAGE IS
OF POOR QUALITY

where $\partial/\partial\bar{n}$ denotes the derivative in the direction of the outward normal from the duct wall. At the entrance plane, the boundary condition is assumed known as

$$p(x,y,0) = G(x,y) \tag{2c}$$

where $G(x,y)$ is a given input pressure. The boundary condition for the exit plane is expressed in the form:

$$\partial p(x,y,d)/\partial z = ik\beta_e p(x,y,d) \tag{2d}$$

The solution to equation (2) can be expressed in the form:

$$p(x,y,z) = \sum_{n=1}^{\infty} [A_n e^{ik_n z} + B_n e^{-ik_n z}]\, F_n(x,y) \tag{3a}$$

in which

$$K_n^2 = k^2 - \lambda_n^2 \tag{3b}$$

$$A_n = \Omega_n/(c_n + 1) \tag{3c}$$

$$B_n = \Omega_n c_n/(c_n + 1) \tag{3d}$$

$$\Omega_n = D_n/\Psi_{nn} \tag{3e}$$

$$D_n = \int_0^{\ell}\int_0^{h} G(x,y)\, F_n(x,y)\, dxdy \tag{3f}$$

$$\psi_{mn} = \int^{\ell}\int F_m(x,y)\, F_n(x,y)\, dxdy\ ,\ (\psi_{mn} = 0\ ,\ m \neq n) \tag{3g}$$

$$c_n = [(K_n/k\beta_e - 1)/(K_n/k\beta_e + 1)]\ e^{2ik_n d} \tag{3h}$$

In equation (3), the characteristic function, F_n, and eigenvalue, λ_n, satisfy the equation

$$\nabla^2 F_n + \lambda_n^2 F_n = 0 \tag{4a}$$

with the condition

$$\frac{\partial F_n}{\partial \bar{n}} - ik\beta F_n = 0 \tag{4b}$$

along the duct perimeter. Note that as indicated in equation (3g), the eigenfunctions satisfying equation (4) are orthogonal. This orthogonality relation has been used in equation (3).

In this paper, equation (4) will be solved by the finite element method. The extracted values of F_n and λ_n can then be substituted into equation (3) to determine the acoustic field. The numerical solution will be used to develop and discuss some of the attenuation characteristics of these peripherally variable liners. Equation (3) is also used to evaluate the effect of a finite termination impedance on the attenuation characteristics in a finite duct.

Attenuation

Before proceeding with the solution to equation (4), it is useful to develop an expression for the attenuation produced by the liner in terms of the parameters which have been introduced. The axial acoustic intensity at any axial position in the duct is

$$I_z = \frac{1}{2\rho_0 ck} \mathrm{Re} \left[-ip^* \frac{\partial p}{\partial z}\right] \tag{5}$$

ORIGINAL PAGE IS
OF POOR QUALITY

where ρ_0 is the ambient density of the medium, Re[ ] denotes the real part of the complex expression enclosed within the brackets and the superscript asterisk indicates the complex conjugate. Furthermore, the total acoustic power is the integral of the acoustic intensity across the cross section

$$E_z = \int_0^h \int_0^\ell I_z dxdy$$

and the decrease in decibels of the acoustic power from $z = 0$ to $z = z_0$ can be written as

$$\Lambda dB = 10 \log_{10}(E_0/E_{z_0}) \tag{6}$$

Generally, the specific acoustic admittance, β, is chosen so as to maximize this attenuation. In terms of the parameters of equation (3), equation (6) becomes

$$\Lambda dB = 10 \log_{10} \frac{R_e[\sum_{m=1}^{\infty} \sum_{n=1}^{\infty} \tilde{\Psi}_{mn} \tilde{A}_{mn}(0)]}{R_e[\sum_{m=1}^{\infty} \sum_{n=1}^{\infty} \tilde{\Psi}_{mn} \tilde{A}_{mn}(z_0)]} \tag{7a}$$

in which

$$\tilde{\Psi}_{mn} = \int_0^\ell \int_0^h F_m F_n^* dxdy \tag{7b}$$

and

$$\tilde{A}_{mn}(z) = k_m(A_m e^{ik_m z} - B_m e^{-ik_m z})(A_n^* e^{-ik_n^* z} + B_n^* e^{ik_n^* z} \tag{7c}$$

Equation (7) will allow calculation of the attenuation produced by the lining in the finite duct.

Variational Formulation

Forsythe and Wasow (ref. 9) show that equation (4) is satisfied if and only if the variational condition

$$\delta \Pi = 0 \tag{8a}$$

where

$$\Pi = \int\int_A [\vec{\nabla}F \cdot \vec{\nabla}F - \lambda^2 F^2]\, dA - ik \int_c \beta F^2 dc \tag{8b}$$

is satisfied. In equation (8), the subscript n on F and λ has been dropped for convenience and $\vec{\nabla}$ is the differential vector operator in the duct cross section. This paper will approach the solution in the duct cross section by using a finite element approximation to the functional Π. This approximate functional, $\bar{\Pi}$, is developed in the next section.

Finite Element Formulation

Finite element discretization. - In the finite element process, the rectangular duct whose cross-section is the region $\{0 \leq x \leq h,\ 0 \leq y \leq \ell\}$, is divided into $(M - 1)\ (N - 1)$ elements as shown in Figure 2. Although many kinds of elements could be used in this setting, attention is restricted to rectangular elements. The width and height of each element are Δy and Δx respectively. Points at the corner of each element, called nodes, are designated as (I, J) where $I = 1, 2, 3, \ldots M$ and $J = 1, 2, 3, \ldots N$. It is at these nodes that the values of the unknown function, F, and its higher derivatives will be determined.

Shape functions. - The finite element technique expands the solution within each element in terms of shape functions. The shape functions at each node are defined in terms of local coordinates

$$\zeta_I = \frac{x - x_I}{\Delta x} \qquad 0 \leq |\zeta_I| \leq 1 \tag{9a}$$

$$\eta_J = \frac{y - y_J}{\Delta y} \qquad 0 \leq |\eta_J| \leq 1 \tag{9b}$$

The shape functions utilized in this analysis, $f_1(\zeta)$ and $f_2(\zeta)$, are even and odd functions, respectively, which are non-zero only in the interval (-1, 1) and which have unit magnitude and slope respectively, at $\zeta = 0$ as illustrated in figure (3). Furthermore, both f_1 and f_2 have zero magnitude and slope at $\zeta = \pm 1$. The functions are

$$f_1(\zeta) = \begin{cases} 1 - 3\zeta^2 + 2|\zeta|\zeta^2 & |\zeta| \leq 1 \\ 0 & |\zeta| > 1 \end{cases} \tag{10a}$$

$$f_2(\zeta) = \begin{cases} \zeta^3 - 2|\zeta|\zeta + \zeta & |\zeta| \leq 1 \\ 0 & |\zeta| > 1 \end{cases} \tag{10b}$$

These functions give the influence of unit magnitude and slope at the node in a one dimensional problem. Thus, the total approximating function may be formed by superimposing functions of this type.

The approximating function for F to be used here is

$$F \simeq C(F_{IJ}^{PQ}) \tag{11a}$$

in which

$$C(T_{IJ}^{PQ}) = \sum_{p=1}^{2} \sum_{Q=1}^{2} \sum_{I=1}^{M} \sum_{J=1}^{N} T_{IJ}^{PQ} f_p(\zeta_I) f_q(\eta_J) \tag{11b}$$

and

$$\begin{bmatrix} T_{IJ}^{11} & T_{IJ}^{12} \\ T_{IJ}^{21} & T_{IJ}^{22} \end{bmatrix} = \begin{bmatrix} T(x_I, y_J) & \Delta y \frac{\partial T}{\partial y}(x_I, y_J) \\ \Delta x \frac{\partial T(x_I, y_J)}{\partial x} & \Delta x \Delta y \frac{\partial^2 T(x_I, y_J)}{\partial x \partial y} \end{bmatrix} \tag{11c}$$

ORIGINAL PAGE IS
OF POOR QUALITY

This expansion insures that the functions F and $\frac{\partial F}{\partial n}$ will be continuous everywhere within the duct and also along its boundaries.

The admittance along the duct perimeter will be similarly expressed in the form

$$\beta \simeq C(\beta_{IJ}^{PQ}) \tag{12}$$

The values of the nodal coefficients in equation (12) are set to zero if node (I, J) does not lie along the duct wall where β is prescribed. Note that the values of the nodal coefficients in the expansion for β (equation (12)) are known whereas those in the function F, equation (11a), will be determined such that the functional, $\overline{\Pi}$, is stationary.

<u>Finite element matrix equations</u>. - The approximating function to F (eq. (11a)) and polynomial representation for β (eq. (12)) lead to an approximate functional $\overline{\Pi}$ which is a quadratic form in the unknown nodal coefficients F_{IJ}^{PQ}

$$\overline{\Pi} = \{F\}^T \left[[S] - ik\,[D] - \lambda^2\,[M]\right] \{F\} \tag{13}$$

where the superscript T indicates the vector transpose. It is convenient to be consistent with the nomenclature used in structural analysis and refer to [S], [D] and [M] as the acoustic stiffness, damping, and mass matrices respectively. [S] and [M] are square symmetric matrices whose coefficients are real. [D] is a complex square symmetric matrix containing the coefficients in equation (12), whereas {F} is an unknown vector containing the coefficients in the expansion given by equation (11a). [S],

[M] and [D] are each of order 4MNX4MN, although many of the entries are zero. The unknown coefficients in {F}, (4MNX1), are ordered so that

$$\{F\}^T = \{F_{11}^{11}, F_{11}^{21}, F_{11}^{12}, F_{11}^{22}, F_{12}^{11}, F_{12}^{21} \ldots F_{MN}\} \tag{14}$$

Requiring that the first variation of the functional vanish leads to a set of matrix equations of the form

$$[[S] - ik[D]]\{F\} = \lambda^2[M]\{F\} \tag{15}$$

Equation (15) may be solved to obtain the eigenvalue λ and eigenvector {F}.

Finite Element Representation of Acoustic Power

In general, the solution to equation (15) will yield many eigenvalues, λ and a different eigenfunction F for each eigenvalue. It is, therefore, convenient to refer to $\{F^n\}$ as the eigenvector corresponding to the eigenvalue λ_n. Now consider the integral ψ_{mn} given by equation (3g). It may be expressed in matrix form as:

$$\psi_{mn} = \{F^m\}^T[M]\{F^n\} \tag{16a}$$

likewise

$$\tilde{\psi}_{mn} = \{F^m\}^T[M]\{F^n\}^* \tag{16b}$$

Further, in order to evaluate the constant D_n (eq. (3f)), expand the boundary condition G(x,y) in the form:

$$G(x,y) = C(G_{IJ}^{pQ}) \tag{17a}$$

D_n is then expressed in the matrix form as:

$$D_n = \{G\}^T[M]\{F_n\} \tag{17b}$$

ORIGINAL PAGE IS
OF POOR QUALITY

in which

$$\{G\}^T = \{G_{11}^{11}, G_{11}^{21}, G_{11}^{12}, G_{11}^{22}, G_{12}^{11}, G_{12}^{21} .. G_{MN}^{22}\} \tag{17c}$$

Equations (16) and (17) allow the determination of the constants A_n and B_n in the solution for the acoustic pressure (eq. (3a)) and the evaluation of the attenuation given by equation (7a). These expressions can then be utilized to evaluate the attenuation of peripherally variable liners.

RESULTS AND DISCUSSION

In this section, the finite element method developed in this paper is first compared to exact analytical solutions for uniform liners. The technique is then exercised to obtain the attenuation characteristics of infinitely long peripherally variable liners. Finally equation (3) is used to evaluate the effects of finite duct termination on the attenuation characteristics of a peripherally variable liner.

For all of these studies, certain parameters were fixed. Finite element results were restricted to four rows and four columns of elements ($M = N = 5$, see fig. 2) with ℓ, h, and d all equal. Modes were ordered according to the imaginary part of the complex propagation constant, K_n. The mode for which the imaginary part of K_n is smallest is referred to as mode one, whereas the mode with the second smallest value is referred to as mode two, etc. Also, the bottom and two side walls of the duct are kept rigid ($\beta_1 = \beta_3 = \beta_2 = 0$) and the eigenfunctions from the numerical and exact analysis are both normalized to unity at the origin.

Uniform Liners

Confidence in the finite element solution may be obtained by showing it compares favorably with exact analytical solutions for uniform liners.

Exact analysis. - When β is constant along each of the four duct walls (fig. 1) the solution to equation 4 is:

$$F_{mn}(x,y) = [\cos \gamma_n x - \frac{ik\beta_3}{\gamma_n}\sin \gamma_n x][\cos \alpha_m y - \frac{ik\beta_1}{\alpha_m}\sin \alpha_m y] \qquad (18a)$$

where the parameters α_n satisfy the trancendental equation

$$[\alpha_n^2 + k^2\beta_1\beta_2] \sin \alpha_n \ell + ik(\beta_1 + \beta_2)\, \alpha_n \cos\alpha_n \ell = 0 \qquad (18b)$$

and the parameters γ_m satisfy the same trancendental equation with $\alpha_n, \beta_1, \beta_2$, and ℓ replaced by $\gamma_n, \beta_3, \beta_4$, and h, respectively. The eigenvalues λ_{mn} are related to α_m and γ_n by the equation

$$\lambda_{mn}^2 = \alpha_m^2 + \gamma_n^2 \qquad (18c)$$

Watson and Lansing (ref. 10) solved the trancendental equation which has the general form of equation (18b) using a Newton-Raphson iterative scheme. This program was used in the present work to extract γ_n and α_m for the results involving uniform liners. These values were also used as a basis for checking the accuracy of the eigenvalues extracted by the finite element method.

Comparison of the numerical and exact analysis. - The first example considered involved calculating eigenvalues for a hard wall duct ($\beta = 0$). The lowest ten eigenvalues from equation 8 are listed under the heading "Exact Eigenvalues" in Table 1. Numerical results are also shown in the table. Good agreement between the finite element and exact eigenvalues is observed. The hard-wall modal integrals ψ_{nn} (eq. 16a) computed by the finite element method are also compared to exact analytical results in table 2. Good agreement is

ORIGINAL PAGE IS
OF POOR QUALITY

again observed.

As a second example, consider a soft wall duct in which $\beta_4 = 2.0 - 1.65i$ and the wave number is unity ($k = 1$). Eigenvalues extracted by the finite element method are compared to those extraxted by a Newton-Raphson iterative scheme in table 3. Good agreement is again obtained. The modal integrals ψ_{nn} for the soft wall duct are also compared to exact analytical values in table 4. Note that good comparison between the exact and analytical values is again obtained.

These two examples of uniform liners illustrate the ability of the finite element approximations presented in this paper to give accurate and reliable results. Although the values are not presented, the modal integrals $\psi_{mn}(m \neq n)$ were also computed for both the hard and soft wall ducts. Both the real and imaginary parts of these integrals were of the order 10^{-4} or less for each of the ten modes considered, indicating that the modes are orthogonal in accordance with equation (3g). It should also be noted that the effects of increasing wave number, k, have not been throughly investigated. However, it has been observed that at least for the first two modes, the error in both the eigenvalues and modal integrals, $\psi_{mn}(m \neq n)$, are consistent with those in the tables for $0 \leq k \leq 10$.

Peripherally Variable Liners

Having established confidence in the finite element solution, this technique is now exercised to obtain the attenuation characteristics of infinitely long peripherally variable liners. The effects of finite duct termination will also be discussed.

Infinitely long peripherally segmented liners. - Extending the approach of Cremer (ref.11), the attenuation characteristics of infinitely long peripheral liners are determined by investigating the attenuation rate of the least attenuated duct mode. The least attenuated mode in the context here shall mean the mode with the smallest attenuation rate. Cremer (ref.11) has determined that, for a two-dimensional infinitely long duct with a hard surface on the lower wall, the attenuation rate of the least attenuated duct mode can be maximized by choosing the admittance of the upper wall to be:

$$\beta_c(kh) = (2.06 - 1.65i)/kh \tag{19}$$

A liner with a wall admittance of $\beta_c(kh)$ is referred to as a Cremer liner and is said to be tuned at k_0 if the admittance of the upper wall is given by $\beta_c(k_0h)$. This relation has been utilized to determine admittance values for the peripherally segmented liners.

In the examples to follow, the bottom and two side walls of the duct in figure 1 have been kept rigid ($\beta_1 = \beta_3 = \beta_2 = 0$). Thus the admittance (see fig. 1) of the upper wall is allowed to vary in a stepwise or continuous fashion. This is at variance with the mathematical models which have been constructed to date which are restricted to axial segmentation of the duct liner (segmentation along the Z-axis).

In order to simplify discussions of peripherally segmented liners, a segmented liner will be referred to as a k_1-k_2-k_3-k_4 liner. This notation implies that:

ORIGINAL PAGE IS
OF POOR QUALITY

$$\beta_4(y) = \begin{cases} \beta_c(k_1 h) & 0 \le y \le \frac{1}{4} \\ \beta_c(k_2 h) & \frac{1}{4} \le y \le \frac{1}{2} \\ \beta_c(k_3 h) & \frac{1}{2} \le y \le \frac{3}{4} \\ \beta_c(k_4 h) & \frac{3}{4} \le y \le 1 \end{cases} \tag{20}$$

where $\beta_c(kh)$ is the Cremer admittance given by equation 19. Also, to avoid referring to a Cremer segment tuned at infinity, the notation $k_1 - 0 - k_3 - k_4$ will denote that the portion of β_4 corresponding to the tuning frequency k_2 is a hard wall.

Numerical studies were conducted to evaluate the effects of shortening the width of an initially full width Cremer liner. Figure 4 illustrates this effect. Note that once a small portion of the liner is taken away, the attenuation rate near the tuning frequency decreases substantially. On first thought, one might expect that by taking away one quarter of the liner, the attenuation rate near the tuning frequency would be reduced by about one quarter. However, in fact the attenuation rate is reduced by about one half.

In figure 5, it can be seen that the attenuation rate of a peripherally segmented liner may also be changed simply by changing the positions of the liner segments. Note, that although the attenuation rate near the tuning frequency of the liner remains the same, the attenuation curve in the mid-frequency range is much broader for a 0-2-0-2 or 0-2-2-0 liner than for a 2-2-0-0 liner.

In figure 6, the attenuation characteristics of peripherally segmented liners having Cremer segments tuned at several frequencies are shown. The first segment of all liners is a Cremer liner tuned at h = 2. It can be seen that the shape of the attenuation curve can be altered, although not substantially, by the variation of the tuning frequencies. Essentially, the curve is dominated by the lowest tuning frequency utilized.

Infinitely long continuous peripheral liners. - The finite element analysis presented in this paper can also be employed to investigate a peripheral liner with continuous variation.

Figure 7 shows the attenuation curves of four peripheral liners with continuous linear variation of the admittance. The admittance β_4 of each liner is given by:

$$\beta_4 = \overline{A}_0 + \overline{A}_1 y \tag{21a}$$

where

$$\overline{A}_0 = \beta_c(2.0\ h) \tag{21b}$$

$$\overline{A}_1 = \beta_c(k_{max}\ h) \tag{21c}$$

ORIGINAL PAGE IS
OF POOR QUALITY

The value of $k_{max}h$ is different for each liner. Note that for each liner the maximum attenuation rate occurs at h = 2. However, the value of this maximum attenuation decreases with increasing $k_{max}h$. There is also some broadening of the attenuation curve at the midfrequencies.

In figure 8, the variation of the real part of the admittance of three different types of liners are compared. The segmented liner is a 2-4-6-8 liner, while the liner with the liner variation has the form of equation 21 with $k_{max}h = 8$. The admittance for the cubic liner was expressed in the form:

$$\beta_4(y) = \bar{A}_0 + \bar{A}_1 y + \bar{A}_2 y + \bar{A}_3 y^3 \tag{22}$$

where the coefficients in equation 22 were chosen to that, at $y = 0$, $y = 1/3$, $y = 2/3$, and $y = 1$, the values of β_{c-4} were $\beta_c(2.0\ h)$, $\beta_c(4.0\ h)$, $\beta_c(6.0\ h)$, and $\beta_c(8.0\ h)$ respectively. The variation of the imaginary part of the admittance of these three liners will be similar to that shown in figure 8.

Figure 9 shows the attenuation rates for each of the three liners. The attenuation rates for the cubic and four-segment liner are not significantly different although the attenuation curve for the cubic liner is slightly broader than that for the segmented liner. The liner with linear variation has a greater attenuation rate than the other two liners in the low to midfrequency range.

Effects of a Termination Impedance on Liner Attenuation

When the duct is of finite length, non-negligible acoustic energy may be carried to the termination by other modes than the least attenuated mode. As a result, the attenuation produced by the liner must be computed from equation 7a, which includes the effect of the termination as well as the interaction between, the different modes. At the present time, the computer

program utilized in this study is unable to compute this equation exactly due to storage limitations. The eigenfunctions , F_n , and modal integrals Ψ_{nn} and $\tilde{\Psi}_{mn}$ must all be retained. In addition, since the subroutine that solves the eigenvalue equations (eq. 15) destroys the mass matrix, the coefficients in this matrix must be stored in another matrix, thus requiring further core.

However, if it is assumed that the source is such that all modes have equal input energy and are in phase and that coupling between the modes can be neglected ($\tilde{\Psi}_{mn} \cong 0$, $m \neq n$), then the attenuation in the finite duct is proportional to the sum of the attenuations of each of the individual modes. Equation 7a reduces in the case of a single mode to:

$$\Delta dB = 10 \, Log_{10} \frac{Re[e^{-2Im(K_n)} - c_n e^{-2iRe(K_n)} + c_n^* e^{2iRe(K_n)} - c_n c_n^* e^{2Im(K_n)}]}{Re[1 - c_n + c_n c_n^*]} \quad (23)$$

Equation 23 is the expression for the attenuation of a single mode in a finite duct. For infinitely long ducts, $c_n = 0$. However, the parameter c_n is not necessarily zero for each mode in the finite duct and thus will affect the value of the attenuation for the mode. Note that c_n(eq. 3h) contains the effect of the termination admittance as well as the duct length, d.

In the remainder of this section, the effects of a $\rho_0 c$ termination impedance ($\beta_e = 1$) upon the attenuation of a single mode in a finite duct will be investigated. Note that since the length of the duct is unity, the expression on the right-hand side of equation 23 may also be referred to as the attenuation "rate". When $c_n \neq 0$, the mode for which the right-

ORIGINAL PAGE IS
OF POOR QUALITY

hand side of equation 23 is smallest will be referred to as the least energy mode. However, when $c_n = 0$, the mode for which the right-hand side of equation 23 is smallest will be referred to as the least attenuated mode.

The attenuation rates for a 2-4-6-8 liner and a 2-2-8-8 liner are given in figures 10 and 11, respectively. In each figure, the attenuation curves for the least energy mode, the least attenuated and the least attenuated mode with reflections ($c_n \neq 0$) are plotted. The asterisk on the attenuation curve for the least energy mode denotes that, at that particular value of kh, the least energy mode is the same as the least attenuated mode. Note that figures 10 and 11 display the same characteristics. The attenuation rate for the least energy mode is less than that of the least attenuated mode with reflections at the lower frequencies. However, each of the three attenuation curves are identical at the higher frequencies. In fact, the least attenuated mode and the least energy mode are the same mode at the higher frequencies.

The results shown on figures 10 and 11 indicate that the termination of the duct must be taken into account in liner optimization studies at the lower frequencies. At the higher frequencies, the attenuation rates are identical indicating that the effects of the termination can be neglected at these frequencies. One should understand however, that these conclusions are based on the assumption that the total attenuation rate in the finite duct is proportional to the attenuation rate of the individual modes.

CONCLUDING REMARKS

Based on the results of this work, the following conclusions are drawn:

1. The attenuation rate for a peripherally segmented liner drops significantly if a small portion of the liner is removed.

2. One can alter the attenuation characteristics of a peripherally segmented liner by placing the liner segments in different positions along the periphery.

3. Based upon the attenuation curves considered here, it appears that the primary effect of peripheral variation is a broadening of the attenuation characteristics for the liner.

4. Effects of the duct termination must be taken into account at the lower frequencies, when optimizing peripherally variable liners.

Conclusions 1, 2, and 3 were based upon infinite ducts, whereas conclusion 4 employed the assumption of equal partition of energy and neglecting coupling for the modes. Although these restrictions are somewhat removed from reality, they do provide a means for investigating the attenuation characteristics of peripherally variable liners.

Future Work

There is additional work to be done with regard to the computer program developed in conjunction with the finite element theory. In order for the computer program to model more realistic ducts, such as finite length ducts with realistic sources, it is suggested that equation 15 be solved out of core. Both matrices are block tridiagonal, symmetric, and in addition [M] and [S] are real. Taking advantage of these special features should allow one to incorporate thousands of degrees of freedom in this present analysis. It is further suggested that the computer program be combined with an optimization program so as to determine if peripherally variable liners can achieve more attenuation than the best uniform liners.

ORIGINAL PAGE IS
OF POOR QUALITY

REFERENCES

1. Nayfeh, A.H.; Kaiser, John E.; and Telinois, Demetri, P.: Acoustics of Aircraft Engine Ducts Systems. AIAA Jour., vol. 13, no. 2, Feb. 1975, pp 130-153.

2. Lansing, D.L.; and Zorumski, W.E.: Effects of Wall Admittance Changes on Duct Transmission and Radiation of Sound. J. Sound & Vib., vol. 27, no. 1, Mar. 8, 1973, pp. 85-100.

3. Zorumski, William E.: Acoustic Theory of Axisymmetric Multisectioned Ducts. NASA TR R-419, 1974.

4. Motsinger, R.D.; Kraft, R.E.; Paas, J.E.; and Gahn, B.M.: Analytical and Experimental Results of Some Segmented Liner Acoustic Performance Studies for High Mach Number Inlets. NASA CR-2882, 1977.

5. Quinn, Dennis W.: Attenuation of the Sound Associated with a Plane Wave in a Multisectional Duct. AIAA Paper No. 75-496, March 1975.

6. Beckemeyer, Roy J.; and Sawdy, David T.: Optimization of Duct Acoustic Liners of Finite Length. Paper H1, 89th Meeting Acoust. Soc. America (Austin, Texas, April 1975.

7. Sawdy, David T.; Beckemeyer, Roy J.; and Patterson, John D.: Optimum Segmented Acoustic Liners for Flow Ducts. Paper D6, 90th Meeting Acoust. Soc. America (San Francisco, CA), Nov. 1975.

8. Lester, Harold; and Posey, Joe W.: Optimum One-Section and Two-Section Circular Sound Absorbing Duct Liners for Plane-Wave and Monopole Sources Without Flow. NASA TN D-8348, 1976.

9. Forsythe, George E.; Wasow, Wolfgang R.: Finite Difference Method for Partial Differential Equations. John Wiley and Sons, Inc., 1960.

10. Watson, Willie R.; and Lansing, Donald L.: A Comparison of Matrix Methods for Calculating Eigenvalues in Acoustically Lined Ducts. NASA TN D-8186, 1976.

11. Cremer, Lothar: Theorie der Luftschall-Dampfund im Rechteckkanal mit schluckender Wand und das sich diabei ergebende hochste Dampfungsmass. Acoustics, vol. 3, no. 2, 1953, pp. 249-263.

TABLE 1

COMPARISON OF EXACT AND FINITE ELEMENT EIGENVALUES FOR A HARD WALL DUCT ($\beta_I = 0$)

MODE NO., n	EXACT EIGENVALUE	EIGENVALUE COMPUTED FROM FINITE ELEMENT METHOD
1	0.000	0.000
2	3.142	3.142
3	3.142	3.142
4	4.443	4.443
5	6.283	6.284
6	6.283	6.284
7	7.025	7.025
8	7.025	7.027
9	8.886	8.887
10	9.425	9.434

TABLE 2

COMPARISON OF EXACT MODAL INTEGRALS WITH THOSE EXTRACTED BY THE FINITE ELEMENT METHOD FOR A HARD WALL DUCT

MODE NO., n	EXACT Ψ_{nn}	VALUE OF Ψ_{nn} COMPUTED FROM FINITE ELEMENT METHOD
1	1.000	1.000
2	.500	.500
3	.500	.501
4	.250	.250
5	.500	.500
6	.500	.495
7	.250	.246
8	.250	.247
9	.250	.245
10	.500	.480

ORIGINAL PAGE IS
OF POOR QUALITY

TABLE 3

COMPARISON OF EIGENVALUES EXTRACTED BY THE FINITE ELEMENT METHOD WITH THOSE OBTAINED BY THE NEWTON-RAPHSON ITERATIVE SCHEME FOR $k = 1$, $\beta_1 = \beta_3 = \beta_2 = 0$ and $\beta_4 = 2.0 - 1.65i$

MODE NO., n	EIGENVALUE COMPUTED FROM NEWTON-RAPHSON ITERATIVE SCHEME	EIGENVALUE COMPUTED FROM FINITE ELEMENT METHOD
1	1.835 - 1.219i	1.834 - 1.218i
2	2.342 - .987i	2.342 - .988i
3	3.487 - .641i	3.484 - .639i
4	3.840 - .602i	3.844 - .602i
5	6.012 - .336i	6.013 - .337i
6	6.440 - .347i	6.432 - .338i
7	6.542 - .348i	6.656 - .351i
8	6.782 - .298i	6.783 - .298i
9	8.693 - .233i	8.696 - .232i
10	9.250 - .217i	9.256 - .218i

TABLE 4

COMPARISON OF THE EXACT MODAL INTEGRALS WITH THOSE COMPUTED BY THE FINITE ELEMENT METHOD FOR THE DUCT OF TABLE 3

MODE NO., n	EXACT Ψ_{nn}	VALUE OF Ψ_{nn} COMPUTED FROM FINITE ELEMENT METHOD
1	-0.823 - 0.282i	-0.081 + 0.282i
2	.164 - .131i	.163 - .131i
3	- .041 + .141i	- .038 + .145i
4	.082 - .066i	.083 - .066i
5	.475 - .027i	.472 - .026i
6	- .041 + .141i	- .025 + .161i
7	.082 - .066i	.088 - .069i
8	.238 - .014i	.237 - .013i
9	.238 - .014i	.232 - .012i
10	.490 - .011i	.472 - .010i

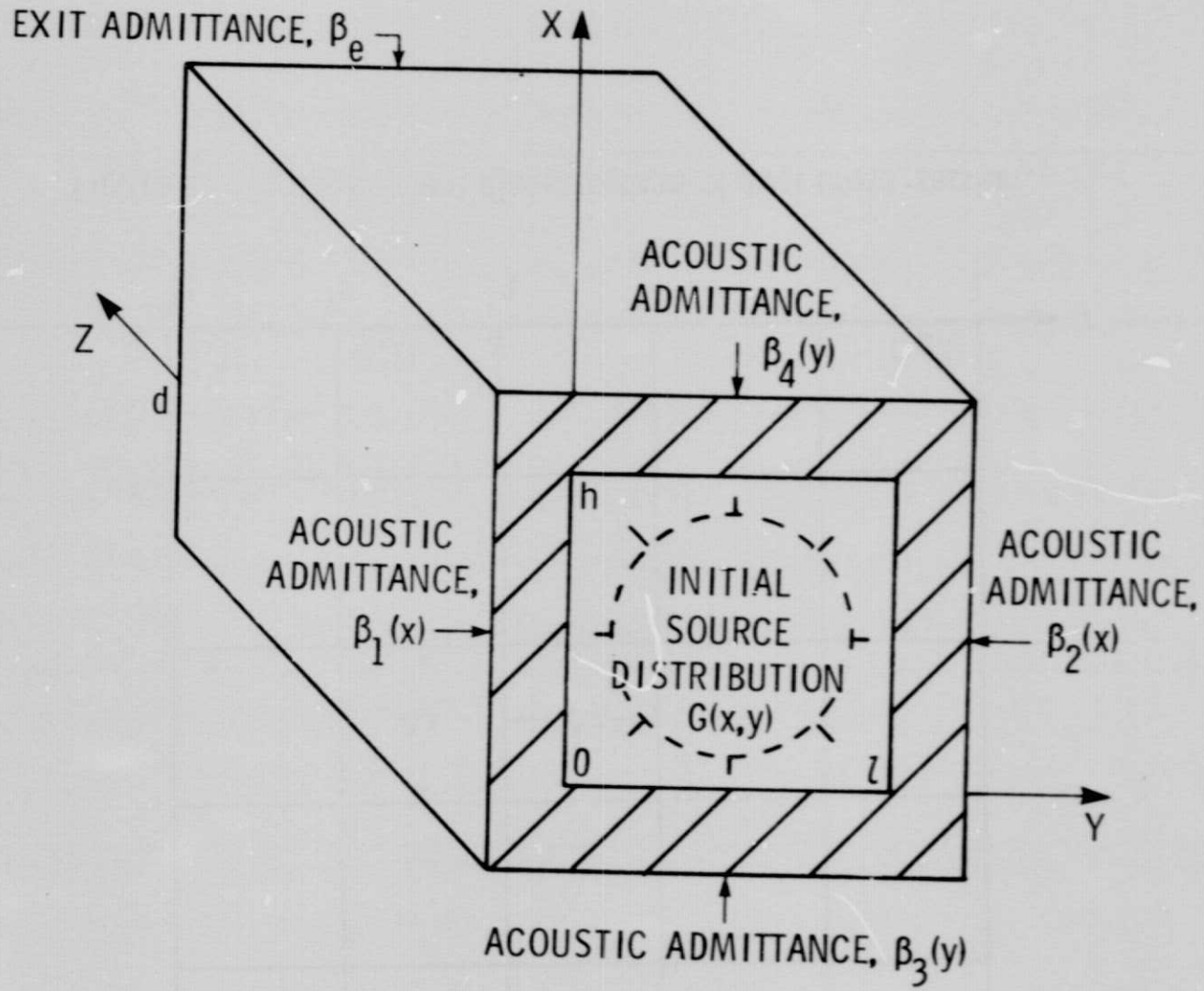

ORIGINAL PAGE IS
OF POOR QUALITY

Figure 1. - Schematic of three-dimensional finite duct with peripherally variable liner.

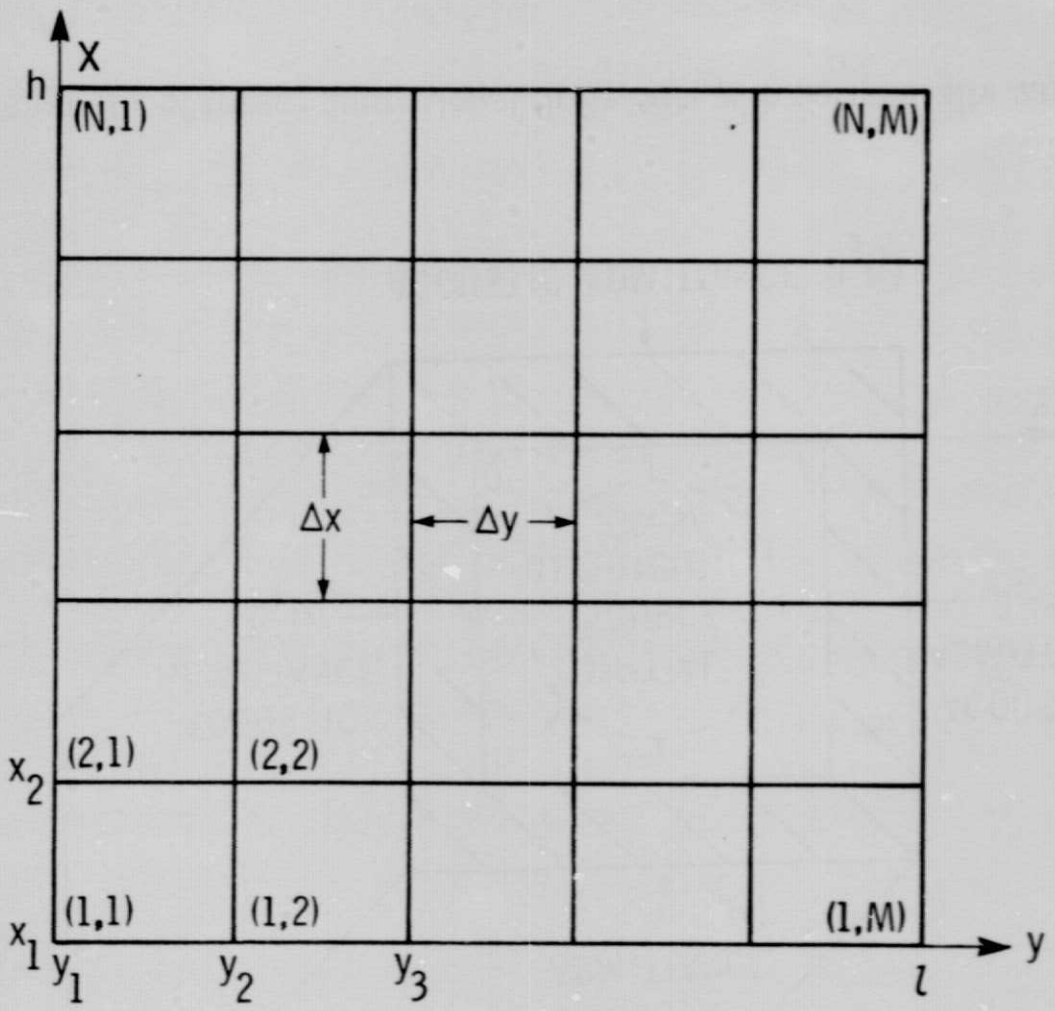

Figure 2. - Finite element discretization of duct cross-section.

ORIGINAL PAGE IS
OF POOR QUALITY

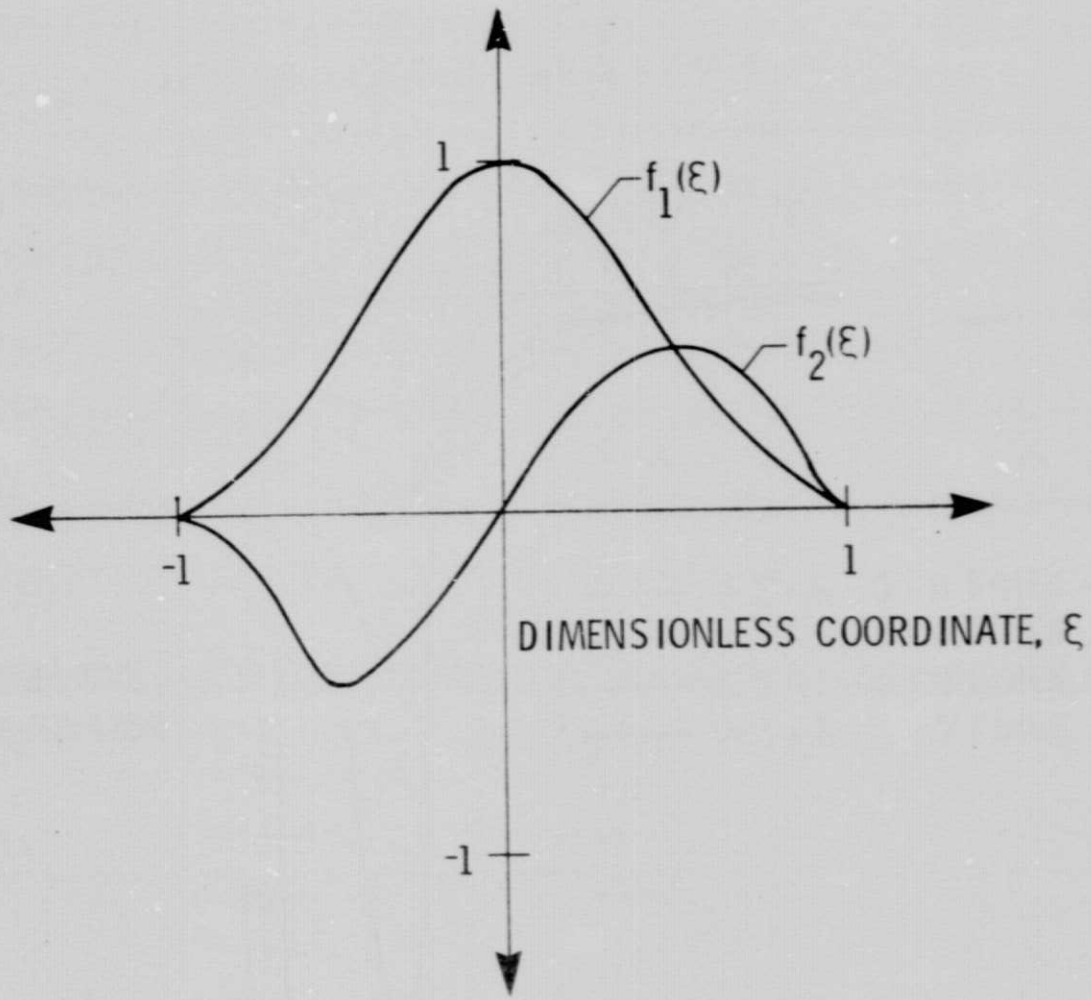

Figure 3. - Cubic shape functions used in finite element approximations.

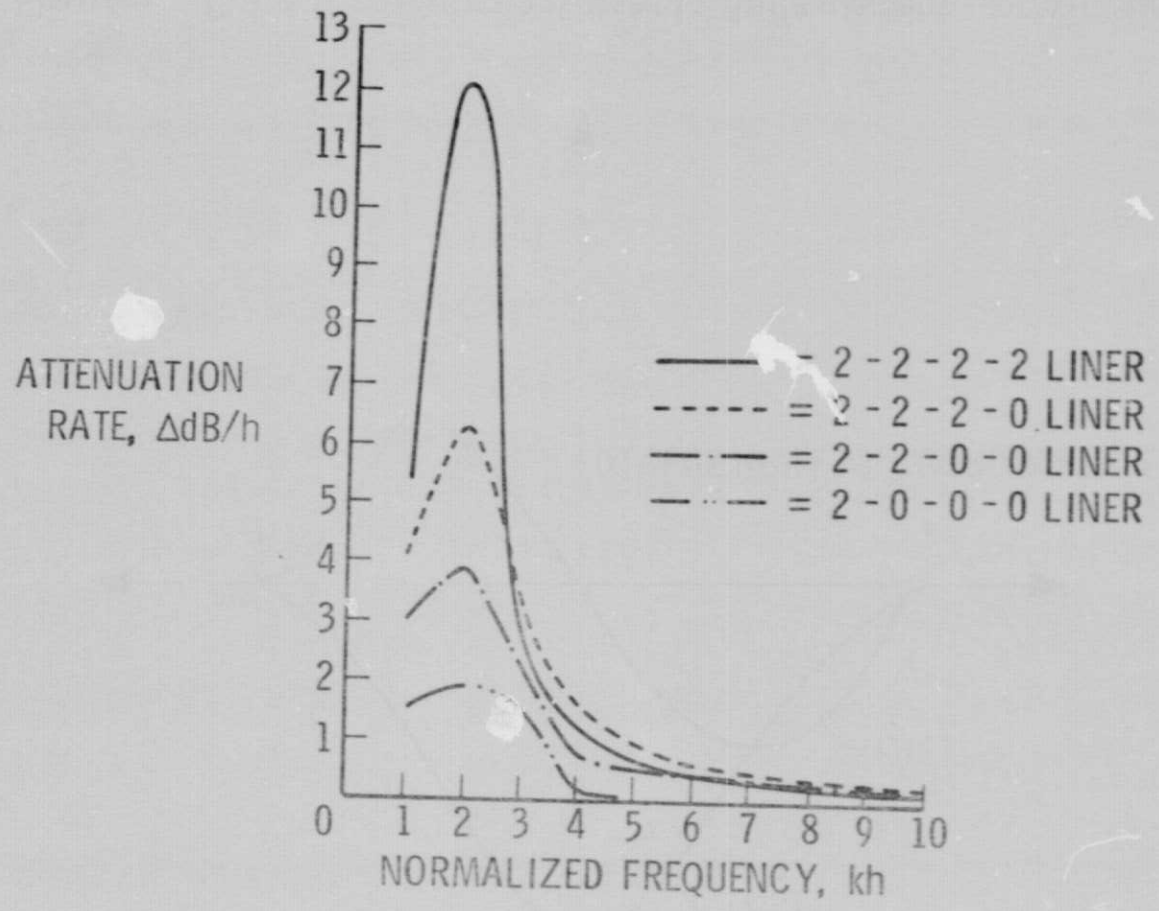

Figure 4. - Effect of width of a segmented liner.

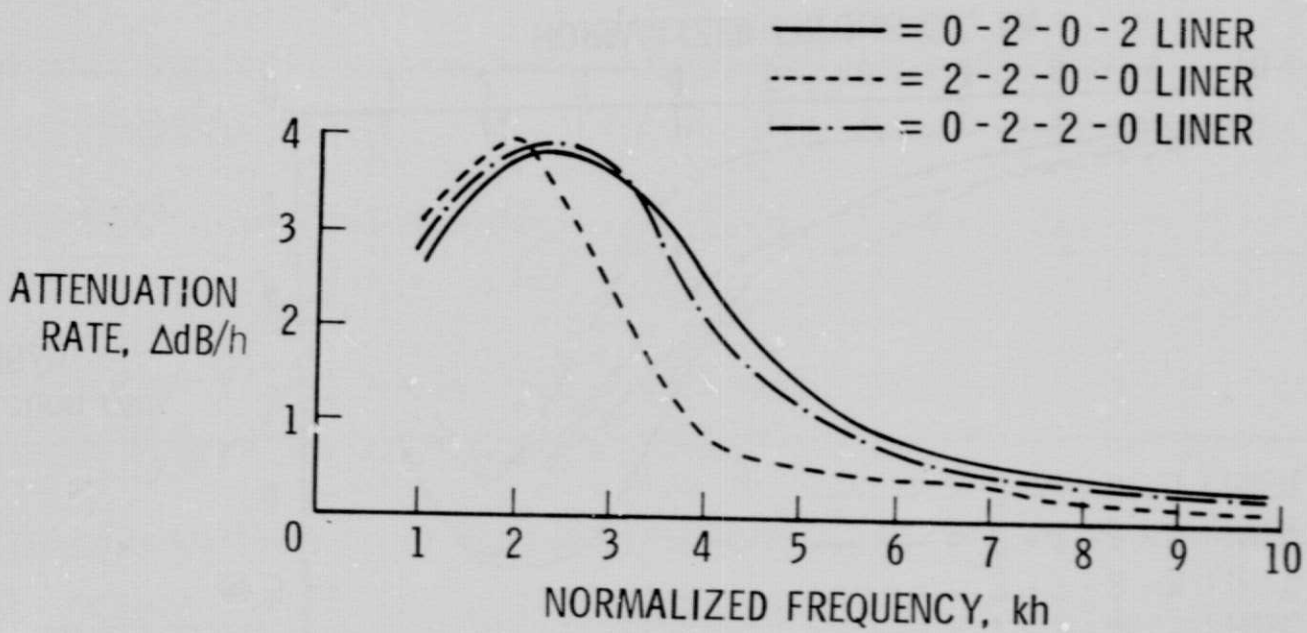

Figure 5. - Effects of positioning of liner segments on the attenuation rate.

ORIGINAL PAGE IS
OF POOR QUALITY

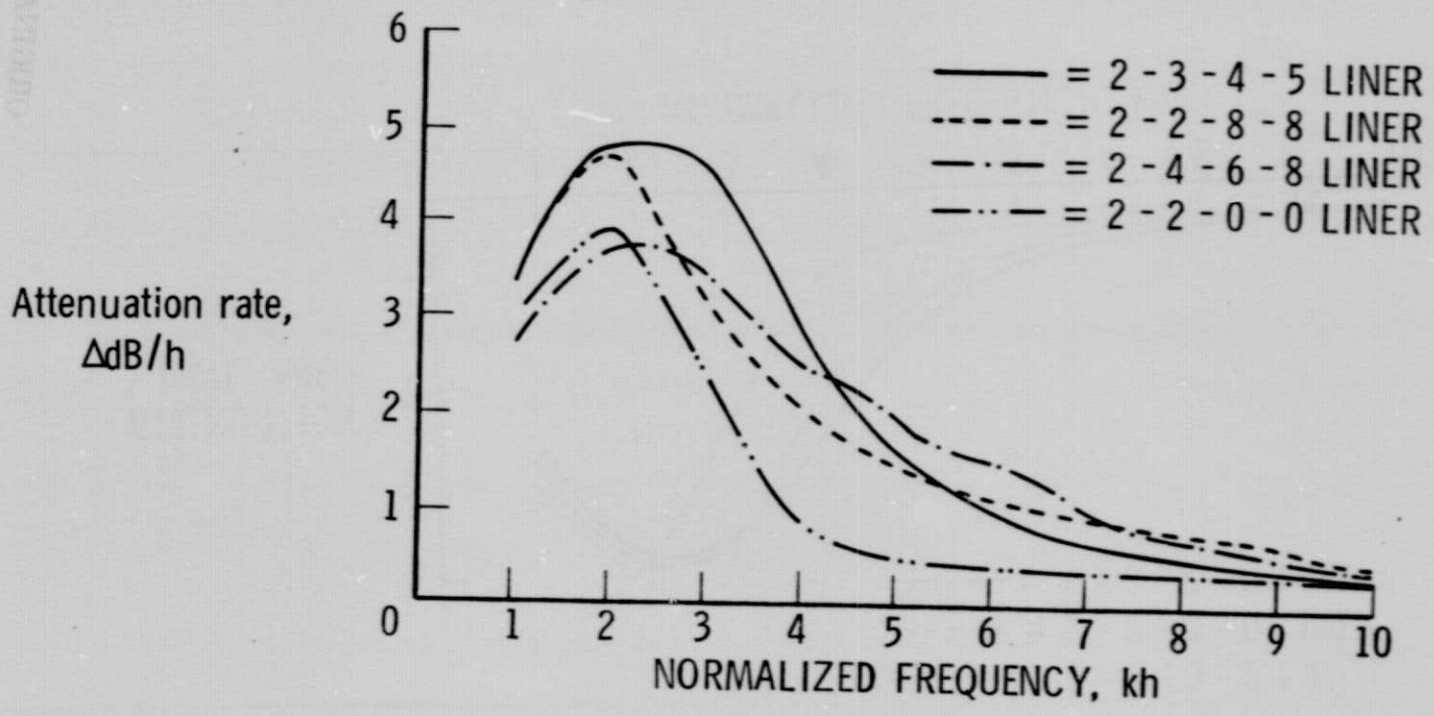

Figure 6. - Attenuation rate of a segmented liner tuned at several frequencies.

ORIGINAL PAGE IS
OF POOR QUALITY

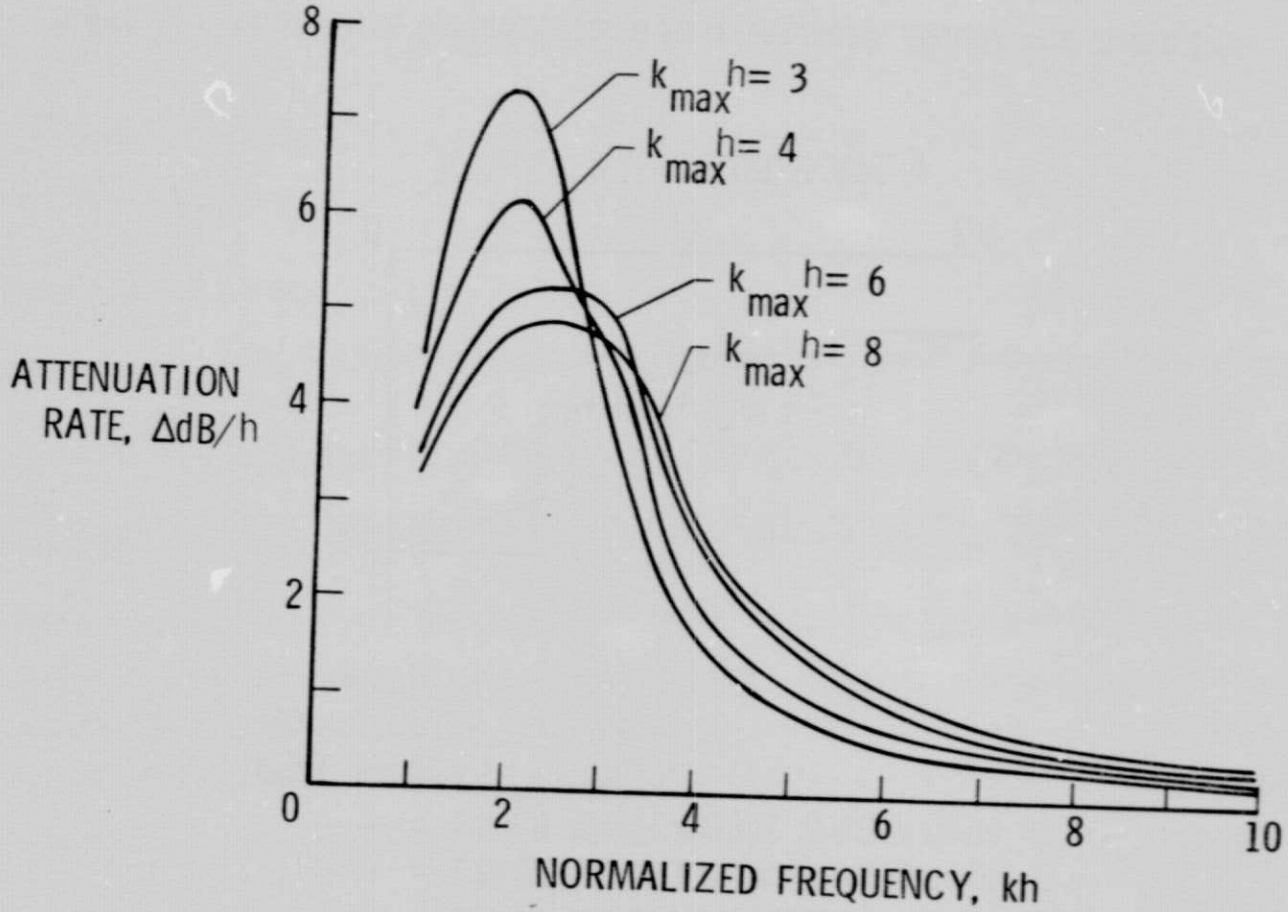

Figure 7. - Attenuation rate of a liner with linear variation of admittance.

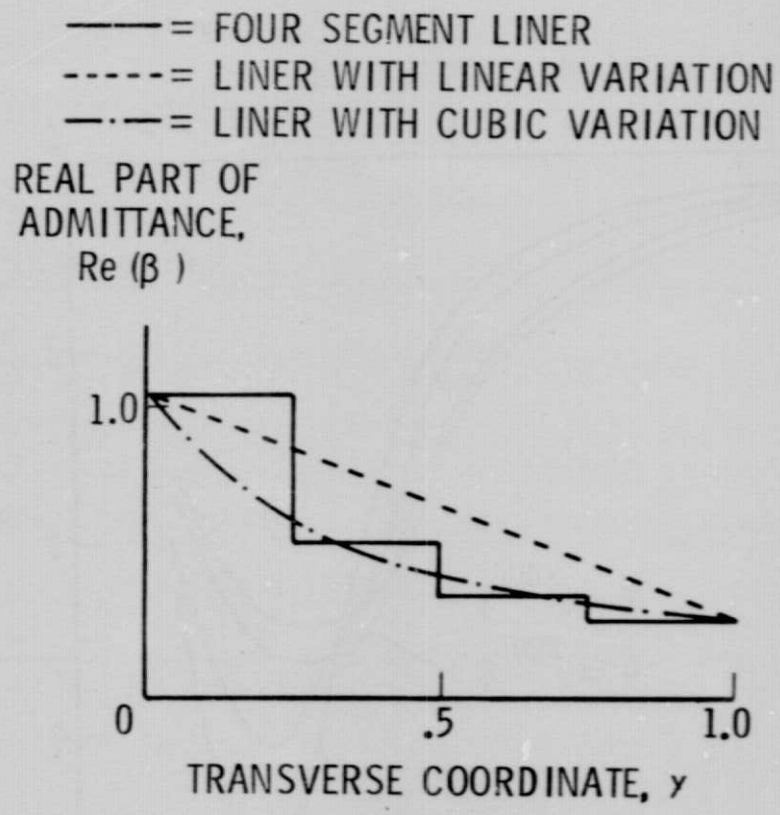

Figure 8. - Admittance variation for a four segment, linear and cubic liner.

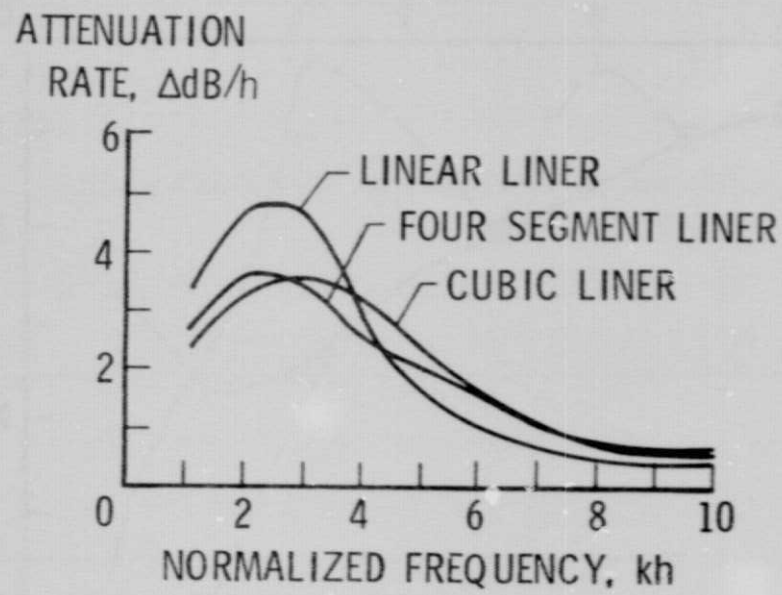

Figure 9. - Attenuation rate for a four segment, linear and cubic liner.

ORIGINAL PAGE IS
OF POOR QUALITY

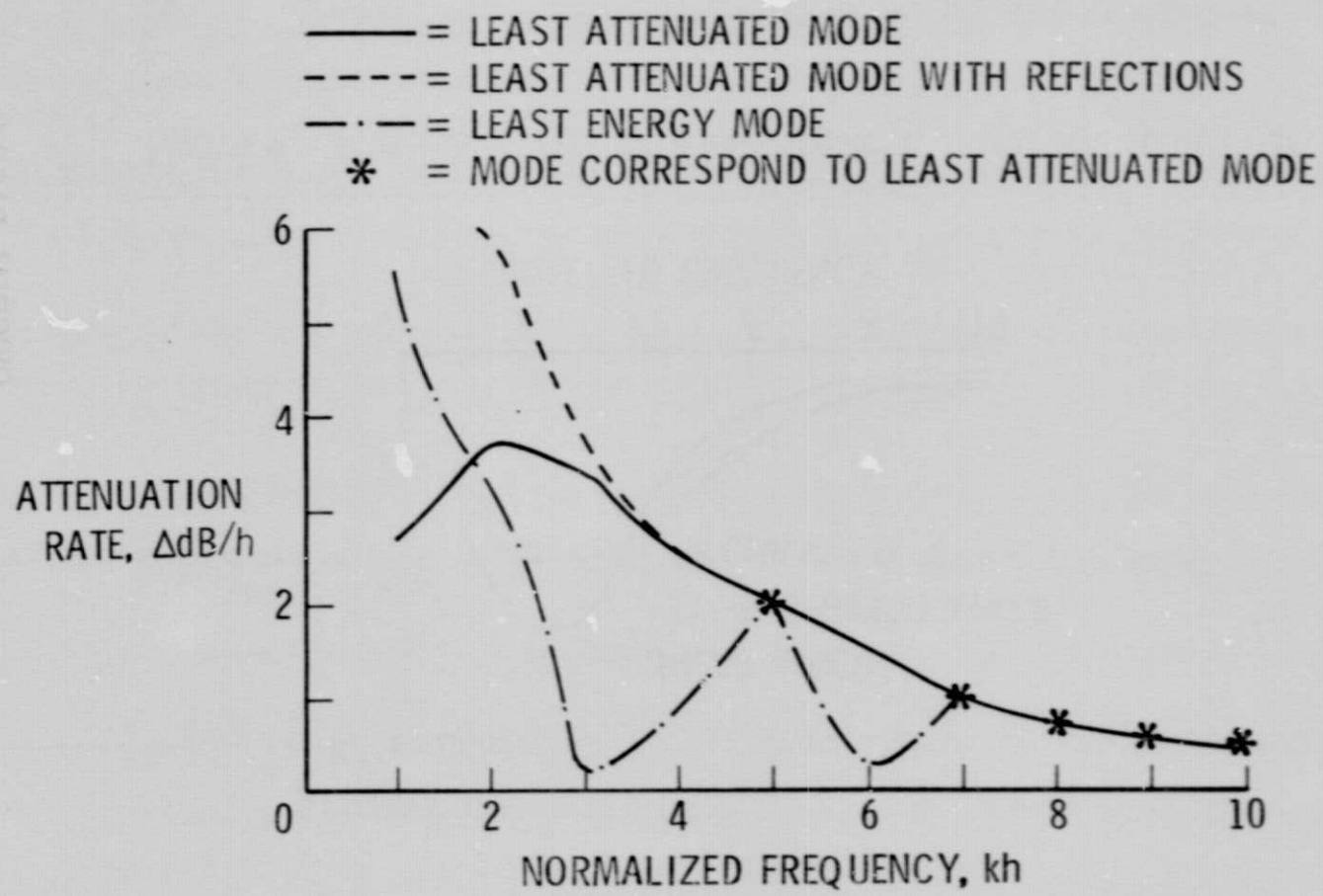

Figure 10. - Attenuation rate in a finite and infinite duct for a 2-4-6-8 liner.

ORIGINAL PAGE IS
OF POOR QUALITY

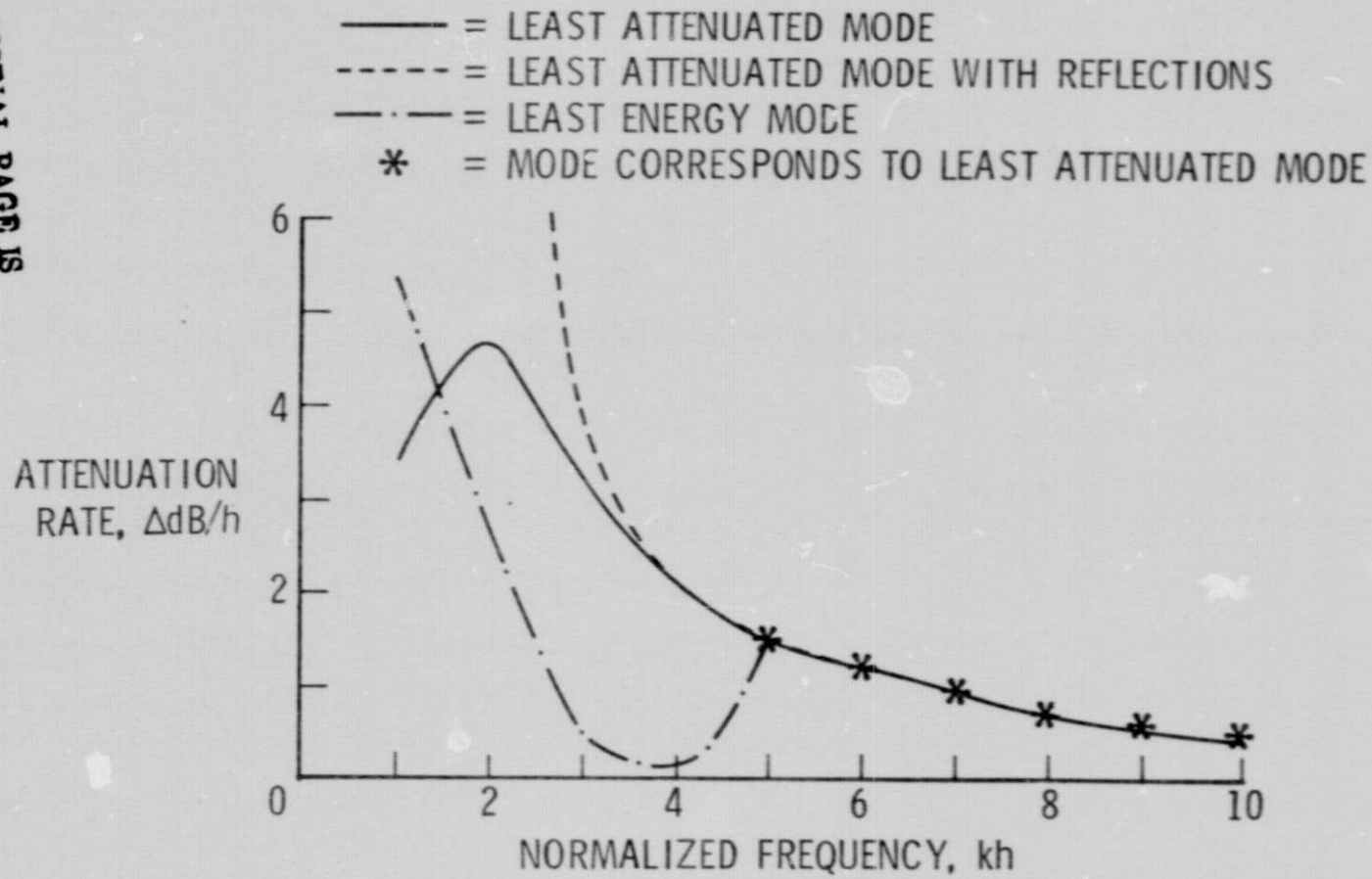

Figure 11.- Attenuation rate in a finite and infinite duct for a 2-2-8-8 liner.

1. Report No.	2. Government Accession No.	3. Recipient's Catalog No.
NASA TM 74080		

4. Title and Subtitle	5. Report Date
A FINITE ELEMENT SIMULATION OF SOUND ATTENUATION IN A FINITE DUCT WITH A PERIPHERALLY VARIABLE LINER?	October 1977
	6. Performing Organization Code: 2640
7. Author(s): WATSON, WILLIE R.	8. Performing Organization Report No.
9. Performing Organization Name and Address: NASA Langley Research Center, Hampton, VA 23665	10. Work Unit No.: 505-03-13-12
	11. Contract or Grant No.
12. Sponsoring Agency Name and Address: National Aeroanutics and Space Administration, Washington, DC 20546	13. Type of Report and Period Covered: Technical Memorandum
	14. Sponsoring Agency Code

15. Supplementary Notes

Basis of paper presented at the 4th Aeroacoustics Conference of AIAA Atlanta, Georgia; October 3-5, 1977.

16. Abstract

Using multimodal analysis, a variational finite element method is presented for analyzing sound attenuation in a three-dimensional finite duct with a peripherally variable liner in the absence of flow. A rectangular element, with cubic shape functions, is employed. Excellent comparison between exact results and the finite element method is obtained in cases where an analytical solution exists. This study indicates that, once a small portion of a peripheral liner is removed, the attenuation rate near the frequency where maximum attenuation occurs drops significantly. Also, it was observed that the positioning of the liner segments affects the attenuation characteristics of the liner and that effects of the duct termination are important in the low frequency ranges. In general, the results indicate that the main effect of peripheral variation of the liner is a broadening of the attenuation characteristics in the mid-frequency range. Finally, it is concluded that, due to matrix size limitations of the presently available computer program, the eigenvalue equations should be solved out of core in order to handle realistic sources.

17. Key Words (Suggested by Author(s))	18. Distribution Statement
Finite element method, duct acoustics and sound attenuation	Unclassified - Unlimited

19. Security Classif. (of this report)	20. Security Classif. (of this page)	21. No. of Pages	22. Price*
Unclassified	Unclassified	39	$4.00

* For sale by the National Technical Information Service, Springfield, Virginia 22161